Chemical analysis of amyloid β aggregation inhibitors derived from Geranium thunbergii

Chemical analysis of amyloid β aggregation inhibitors derived from *Geranium thunbergii*

Kenji Kubo[1], Hikaru Watanabe[1], Hiroyuki Kumeta[2], Tomoyasu Aizawa[2], Chigusa Seki[1], Hiroto Nakano[1], Kiyotaka Tokuraku[1], Koji Uwai[1*]
[1]Graduate School of Engineering, Muroran Institute of Technology,
27-1Mizumoto-cho, Muroran, Hokkaido 050-8585, JAPAN
[3]Graduate Schol of Life Science, Hokaido University, Kita 10, Nishi 8, Kita-ku, Saporo, Hokaido 060-0808, JAPAN

*Correspondence:
Dr. Koji Uwai
Division of Sustainable and Environmental Engineering, Graduate School of Engineering, Muroran Institute of Technology, 27-1 Mizumoto, Muroran 050-8585, Japan
e-mail: uwai@mmm.muroran-it.ac.jp

Abbreviations
AD, Alzheimer's disease; Aβ, amyloid beta; STD-NMR, saturation transfer difference-nuclear magnetic resonance; EtOH ext., ethanol extract; AcOEt, ethyl acetate; MeOH, methanol; EtOH, ethanol; $CHCl_3$, chloroform; CH_3CN, acetonitrile; EC_{50}, half-maximal effective concentration; Fr., fraction.

Abstract

Amyloid β (Aβ) aggregates in the brains of patients with Alzheimer's disease (AD) and accumulates via oligomerization and subsequent fiber elongation processes. These toxicity-induced neuronal damage and shedding processes advance AD progression. Therefore, Aβ aggregation-inhibiting substances may contribute to the prevention and treatment of AD. We screened for Aβ42 aggregation inhibitory activity using various plant extracts and compounds, and found high activity for a *Geranium thunbergii* extract (EC_{50} = 18 μg/mL). Therefore, we screened for Aβ42 aggregation inhibitors among components of a *G. thunbergii* extract and investigated their chemical properties in this study. An active substance was isolated from the ethanol extract of *G. thunbergii* based on the Aβ42 aggregation inhibitory activity as an index, and the compound was identified as geraniin (**1**) based on spectral data. However, although geraniin showed *in vitro* aggregation-inhibition activity, no binding to Aβ42 was observed via saturation transfer difference-nuclear magnetic resonance (STD-NMR). In contrast, the hydrolysates gallic acid (**2**) and corilagin (**5**) showed aggregation-inhibiting activity and binding was observed via STD-NMR. Therefore, the hydrolysates produced under the conditions of the activity test may contribute to the Aβ42 aggregation-inhibition activity of *G. thunbergii* extracts. Geraniin derivatives may help prevent and treat AD.

Keywords

Alzheimer's disease, amyloid-beta, *Geranium thunbergii,* geraniin, saturation transfer difference - nuclear magnetic resonance, amyloid β aggregation inhibitor, hydrolysis.

1. Introduction

Alzheimer's disease (AD) is one of the most common neurodegenerative diseases that occurs during late adulthood and accounts for 70% of dementia cases. The onset of AD leads to the progressive loss of learning ability and decline in mental, behavioural, and functional capacity.[1] Based on accelerating aging in various demographics, the incidence of AD is estimated to reach 150 million by 2050.[2] Choline esterase inhibitors (donepezil, galanthamine, and rivastigmine) and an *N*-methyl-D-aspartic acid receptor antagonist (memantine) are currently used to treat AD. However, these treatments can only slow the progression of AD.[3] Therefore, the development of basic AD treatments and preventive measures during daily life is necessary.

Amyloid plaque and neurofibrillary tangles represent important pathological features of AD. AD onset is thought to be triggered by an increase in production of amyloid β (Aβ) via a missense mutation in the amyloid precursor protein, pre-serin 1, and pre-serin 2 genes in the brain. This Aβ monomer aggregates to form Aβ oligomers and Aβ fibers, which are deposited as amyloid plaques; these neurotoxicities affect the function of synapses and nerve cells. Furthermore, ion channels are blocked in nerve cells, homeostasis is disrupted, and nitric oxide synthase is activated, and oxidation, nitrogenation stress, and mitochondrial damage occur. In addition, kinases and phosphatases are activated, which promote abnormal phosphorylation of tau protein and create neurofibrillary tangles. Consequently, cell death may occur owing to dysfunction of nerve cells and loss of transmitters over a wide area, following AD development (amyloid cascade hypothesis).[4] Previous studies have

investigated approaches to prevent or treat AD using small molecules that specifically and efficiently inhibit Aβ aggregation. Small molecule polyphenols have been reported to exhibit Aβ aggregation inhibitory activity.[5] Since the interaction of these polyphenols with the aromatic amino acid residue of Aβ is involved in the inhibition of Aβ aggregation, the strength of the interaction varies with the structure of the polyphenol.[5] In addition, since plants represent a rich source of polyphenols, it is expected that new Aβ aggregation-inhibiting active polyphenols can be isolated from plants.

To date, we have screened for various natural product extracts and compounds to identify Aβ aggregation-inhibiting natural sources and substances.[6–10] We found that the plant extract of *Geranium thunbergii* (Thunberg's geranium) showed high Aβ aggregation-inhibiting activity (half-maximal effective concentration [EC_{50}] = 4 □g/mL) compared with that of *Mentha spicata* (spearmint; EC_{50} = 18 □g/mL) as the reference value for activity.

G. thunbergii is a perennial herb of the Geraniaceae family, which is distributed in Japan, the Korean Peninsula, and mainland China, and represents a crude drug for treating stagnation and intestinal regulation.[11] Presently, approximately 50–70% of the components present in *G. thunbergii* are tannins, and 20 different types of components, including the main component elaeocarpusin, have been identified.[12–21] Among them, geraniin and corilagin, which are substances related to cognitive function, inhibit β-secretase activity *in vitro*.[14] The purpose of this study was to isolate and characterize Aβ aggregation inhibitors derived from *G. thunbergii* to identify drug candidates for the prevention of dementia.

2 Material and Methods

2.1 Chemistry

2.1.1 General

The CHROMATOREX ODS DM1020T (Fuji Silysia Chemical, Kasugai, Japan) was used in reverse-phase column chromatography. For thin-layer chromatography (TLC) analysis, Silica gel 60 RP18 F254s (Merck-Millipore, Darmstadt, Germany) was used and UV absorption was detected using Handy UV Lamp SLUV-4 254 nm (AS ONE Corporation, Osaka, Japan). Anisaldehyde-sulphuric acid reagent was used in TLC analysis to develop color upon heating. The JEOL JMN-ECA-FT-500 nuclear magnetic resonance (NMR) system was used for NMR spectrum measurement. For ^{1}H-NMR spectrum measurement, the $(CD_3)_2CO$ signal was based on 2.04 ppm and the heavy water (D_2O) signal was based on 4.65 ppm. The coupling constant (*J*) is represented by hertz (Hz), the chemical shift value is represented by δ (ppm), and the coupling mode was as follows: singlet: s, doublet: d, doublets of double: dd, triplet: t, multiplete: indicated as m. For the measurement of the ^{13}C-NMR spectrum, the $(CD_3)_2CO$ signal was based on 29.8 ppm. Saturation transfer difference (STD) NMR was performed using a Bruker Avance III HD 600 MHz spectrometer (Bruker, Billerica, MA, USA). Shimadzu GCMS-QO2010 SE was used for electron ionization-mass spectrometry analysis, and the measurement was performed by direct introduction. Ethyl acetate (AcOEt), methanol (MeOH), ethanol (EtOH), chloroform ($CHCl_3$), $(CH_3)_2CO$, acetonitrile (CH_3CN), dimethyl sulphoxide (DMSO) were purchased from Kanto Chemical (Tokyo,

Japan). Ultrapure water involved distilled water obtained from tap water purified using Autostill WG23 (Yamato Scientific, Tokyo, Japan) and ultrapure water purified using Milli-Q (Merck-Millipore). Gallic acid and ellagic acid were purchased from Tokyo Chemical Industry (Tokyo, Japan). Corilagin was purchased from Sigma–Aldrich (St. Louis, MO, USA).

2.1.2 Fractionation of Aβ aggregation inhibitor derived from *G. thunbergii*

Whole plant material of *G. thunbergii* (43.0 g) was collected from Shiranuka town, Hokkaido, Japan (43°08'11"N, 144°01'22"E) in August 2017, and was extracted using EtOH (215 mL) at room temperature（15～25℃） for 1 week and dried under reduced pressure to obtain a plant extract (1.29 g). The plant extract (1.29 g) was liquid–liquid partitioned using $CHCl_3$, AcOEt, and H_2O, of which the AcOEt phase (253 mg) was adsorbed onto celite (759 mg) and subjected to reverse-phase column chromatography (18.1 cm^3). The fractions Fr. 1-1 (22.9 mg), Fr. 1-2 (89.4 mg), Fr. 1-3 (22.4 mg), and Fr. 1-4 (58.2 mg) were obtained via elution using H_2O/CH_3CN (80:20; *v*/v), and Fr. 1-5 (43.7 mg) was obtained using CH_3CN. Fr. 1-2 and 1-3 (112 mg) were subjected to reverse-phase column chromatography (20.0 cm^3), after which Fr. 2-1 (6.14 mg) and Fr. 2-2 (76.3 mg) were obtained via elution using H_2O/CH_3CN (82:18; *v*/*v*), and Fr. 2-3 (18.9 mg) was obtained using CH_3CN. Fr. 2-2 (76.3 mg) was precipitated using CH_3CN-H_2O to obtain Gt. 1 (65.2 mg) and a filtrate (12.0 mg).

2.1.3 Structural analysis of active substance: Geraniin (**1**)

Compound 1 (65.2 mg), a yellowish solid, was obtained from *G. thunbergii.*

^{1}H-NMR (500MHz, $(CD_3)_2CO$) Form A δ□7.20 (s, 2H), 7.18 (s, 1H), 7.13 (s, 1H), 6.63 (s, 1H), 6.53, (bs, 1H), 6.52 (s, 1H), 5.55 (bs, 1H), 5.51 (bs, 1H), 5.50 (bs, 1H), 5.15 (s, 1H), 4.94 (bs, 1H), 4.78 (bs, 1H), 4.28 (dd, 1H, *J* = 12.3, 2.6). Form B δ□7.25 (s, 1H), 7.19 (s, 2H), 7.08 (s, 1H), 6.62 (s, 1H), 6.55, (bs, 1H), 6.24 (d, 1H, *J* = 1.4), 5.59 (bs, 1H), 5.57 (bs, 1H), 5.42 (bs, 1H), 4.93 (s, 1H), 4.78 (bs, 1H), 4.75 (bs, 1H), 4.40 (dd, 1H, *J* = 8.4, 2.3). ^{13}C-NMR (125MHz, $(CD_3)_2CO$) Form A δ□191.8, 168.3, 166.1, 165.6, 165.4, 164.7, 154.7, 146.0, 145.8, 145.5, 145.1, 145.0, 144.6, 143.5, 139.8, 138.9, 137.9, 136.5, 128.6, 125.7, 124.8, 120.3, 119.7, 117.0, 115.8, 115.2, 113.4, 111.0, 110.6, 108.0, 96.3, 92.5, 90.7, 72.6, 69.9, 66.0, 63.7, 63.3, 46.3. Form B δ□194.5, 168.2, 166.1, 165.7, 164.8, 164.7, 149.3, 147.7, 147.3, 146.0, 145.4, 145.2, 145.0, 144.7, 139.7, 137.8, 137.4, 136.5, 125.5, 125.0, 124.6, 120.3, 120.2, 117.2, 116.8, 115.1, 113.3, 110.7, 110.3, 109.2, 108.7, 92.4, 91.8, 73.3, 70.5, 67.0, 63.8, 62.4, 52.0. ESI-MS *m/z* = 951.4 $[M-H]^-$ for $C_{41}H_{28}O_{27}$.

All of the spectral data of the compounds were in agreement with reported values for geraniin (**1**).[22]

2.2 Biological assays and mechanism of action

2.2.1 Microliter-scale high throughput screening (MSHTS) system

An MSHTS system was established as described previously.[6] Various concentrations of rosmarinic acid derivatives, 30 nM QD-labeled Aβ(1-40) (QDAβ(1-40)), and 30 μM Aβ(1-42) in phosphate-buffered saline (PBS) containing 5% EtOH and 3% DMSO were incubated in a 1,536-well plate at

37 °C for 24 h, and the QDAβ(1-40)–Aβ(1-42) co-aggregates formed in each well were evaluated using an inverted fluorescence microscope equipped with a color CCD camera (DP72, Solutions Corp., Tokyo, JAPAN). SD values of fluorescence intensities of 10,000 pixels (100 × 100 pixels: 167 × 167 mm) in the central region of each well were measured using the ImageJ software (National Institutes of Health, Bethesda, MD, USA). The SD values, which were approximately proportional to the amount of the aggregates, were plotted against the concentrations of added rosmarinic acid derivatives to generate an inhibition curve. EC_{50} values were estimated from the inhibition curve using the EC_{50} shift function in the GraphPad Prism 6 (GraphPad software, San Diego, CA, USA).

2.2.2 Thioflavine T (ThT)-based detection

The ThT method was performed as described previously.[23] Briefly, the test compounds were diluted using an assay buffer (10% EtOH, 1× PBS), and 5 □L of a diluted solution of 600, 60, 6, 0.6, 0.06, and 0 □M was prepared, 3 points each (sample solution). 1 mM Aβ (in DMSO as a storage solution) was diluted to 60 □M Aβ(1-42) with 1× PBS, and 5 □L of the solution was added to each sample solution (final concentration: 30 □M Aβ (1-42), 1× PBS, 5% EtOH, 3% DMSO). The Aβ complex adhered to the tube wall was detached via centrifugation (flash) (Prism Mini, Labnet, Edison, NJ, USA) and dropped to the bottom of the tube, following incubation at 37 ºC for 24 h. Subsequently, 190 μL of the ThT solution (5 □M ThT in 50 mM glycine-NaOH buffer (pH 8.5)) was added to 10 □L of sample solution. A black microfluorescent cell (FM20B-B-25; GL Science, Tokyo, Japan) was used for determining the fluorescence intensity (G-4500, Hitachi, Tokyo, Japan). In the fluorescence measurement, the excitation and fluorescence wavelengths were 455 nm and 490 nm, respectively. From the measured fluorescence intensity, GraphPad Prism 6 (GraphPad software, San Diego, CA, USA) nonlinear regression (Curve fit), Asymmetric Sigmoidal, 5PL, X is log (concentration) was used to calculate the EC_{50} values for aggregation inhibition.

2.2.3 Degradation of geraniin under assay conditions for Aβ aggregation inhibitory activity

An NMR solution was prepared to contain the same conditions as those in the MSHTS analysis. First, D_2O was used to prepare a 10× PBS solution. Next, each sample (final concentration: 1.0 mM) was dissolved in 32 μL of CD_3CD_2OD, following addition of 530 μL of D_2O and 65 μL of 10× PBS. Aβ dissolved in 19 μL $(CD_3)_2SO$ was added, and the ^{1}H-NMR spectrum was measured and used as the 0-hour spectrum. Incubation was performed at 37 °C for 24 h, and the ^{1}H-NMR spectrum was measured and used as the 24-hour spectrum.

2.2.4 Geraniin hydrolysis and decomposition products

An NMR solution was prepared to contain the various conditions modified the MSHTS analysis. Sample was measured in various conditions as follows: 1): D_2O, 2): 5% CD_3CD_2OD in 9.6 mM PBS with 1.0 mM geraniin, 3) 5% CD_3CD_2OD in 5 mM PBS with 1.0 mM geraniin). The ^{1}H-NMR spectrum was measured and used as the 0-hour spectrum. Incubation was performed at 0°C or 37 °C for 24 h, and the ^{1}H-NMR spectrum was measured and used as the 24-hour spectrum.

2.2.5 Comparison of proton nuclear magnetic resonance spectra between hydrolysates of geraniin

An NMR solution was prepared to contain the same conditions as those in the MSHTS analysis without Aβ (5% CD_3CD_2OD, 3% $(CD_3)_2SO$ in 1×PBS with 1.0 mM samples. ^{1}H-NMR spectrum was measured and used as the 0-hour spectrum. Incubation was performed at 37 °C for 24 h, and the ^{1}H-NMR spectrum was measured and used as the 24-hour spectrum.

geraniin (1): 0 hr incubation

^{1}H-NMR (500 MHz, 5% CD_3CD_2OD, 3% $(CD_3)_2SO$ / 1×PBS) Form A δ 7.22 (s, 1H), 6.97 (s, 2H), 6.44 (s, 1H), 6.27 (bs, 1H), 6.23 (bs, 1H), 6.19 (bs, 1H), 5.45 (bs, 1H), 4.92 (bs, 1H), 4.32 (bs, 1H), 4.09 (t, 1H, *J* =8.7). Form B δ 7.13 (s, 1H), 7.03 (s, 2H), 6.82 (s, 1H), 6.54 (s, 1H), 5.36 (bs, 1H), 5.32 (bs, 1H), 4.82 (bs, 1H), 4.25 (t, 1H, *J* =9.5).

geraniin (1): 24 h incubation

^{1}H-NMR (500 MHz, 5% CD_3CD_2OD, 3% $(CD_3)_2SO$ / 1×PBS) δ 7.36 (s, 1H), 7.20 (s, 8H), 7.12 (s, 3H), 7.07 (s, 2H), 7.03 (s, 4H), 7.01 (s, 10H), 7.00 (s, 9H), 6.99 (s, 2H), 6.98 (s, 15H), 6.97 (s, 3H), 6.96 (s, 6H), 6.95 (s, 11H), 6.84 (s, 1H), 6.79 (s, 4H), 6.76 (s, 4H), 6.65 (s, 2H), 6.64 (s, 6H), 6.62 (s, 2H), 6.62 (s, 2H), 6.61 (s, 2H), 6.60 (s, 4H), 6.58 (s, 4H), 6.55 (s, 1H), 6.47 (s, 3H), 6.44 (s, 3H), 6.28 (bs, 11H), 6.23 (s, 3H), 6.20 (s, 6H), 6.19 (s, 2H), 5.57 (s, 10H), 5.49 (s, 3H), 5.44 (s, 9H), 5.40 (s, 3H), 5.34 (s, 7H), 5.22 (s, 4H), 5.16 (s, 3H), 5.00 (s, 5H), 4.91 (s, 3H), 4.51 (t, 6H, *J* =9.6), 4.38 (s, 7H), 4.23 (m, 9H), 4.15 (s, 7H), 4.12 (s, 10H), 4.10 (dd, 6H, *J* =7.6, 2.9).

gallic acid (2): 0 h incubation

^{1}H-NMR (500 MHz, 5% CD_3CD_2OD, 3% $(CD_3)_2SO$ / 1×PBS) δ 6.90 (s, 2H).

gallic acid (2): 24 h incubation

^{1}H-NMR (500 MHz, 5% CD_3CD_2OD, 3% $(CD_3)_2SO$ / 1×PBS) δ 6.89 (s, 2H).

ellagic acid (3): 0 h incubation

^{1}H-NMR (500 MHz, 5% CD_3CD_2OD, 3% $(CD_3)_2SO$ / 1×PBS) δ 7.80 (s, 1H), 7.39 (s, 1H).

ellagic acid (3): 24 h incubation

^{1}H-NMR (500 MHz, 5% CD_3CD_2OD, 3% $(CD_3)_2SO$ / 1×PBS) δ 7.79 (s, 3H), 7.39 (s, 2H).

corilagin (5): 0 h incubation

^{1}H-NMR (500 MHz, 5% CD_3CD_2OD, 3% $(CD_3)_2SO$ / 1×PBS) δ 6.92 (s, 2H), 6.63 (s, 1H), 6.52 (s, 1H), 6.15 (s, 1H), 4.45 (t, 1H, *J* =9.1), 4.34 (d, 1H, *J* =2.7), 4.08 (bs, 1H), 4.03 (dd, *J* =9.1, 2.7).

corilagin (5): 24 h incubation

^{1}H-NMR (500 MHz, 5% CD_3CD_2OD, 3% $(CD_3)_2SO$ / 1×PBS) δ 6.90 (s, 2H), 6.60 (s, 1H), 6.52 (s, 1H), 6.14 (s, 1H), 4.44 (t, 1H, *J* =8.3), 4.33 (bs, 1H), 4.07 (bs, 1H), 4.03 (dd, *J* =8.3, 1.7).

2.2.6 STD NMR

STD-NMR analyses were performed using a Bruker Avance III HD 600 MHz spectrometer at 278 K, which was equipped with a triple resonance ^{1}H, ^{13}C, and ^{15}N probe. Chemical shifts are presented in ppm with respect to the 0 ppm point of the manufacturer's indirect referencing method. The STD

experiments were recorded (number of scans: 4,096) using the sequence proposed by Meyer and co-workers.[24] A cascade of Gaussian-shaped pulses of 50 ms with a power level of -12.79 dB was used for the 2.0 s saturation time. The on resonance irradiation was performed at -0.3 ppm, while the off resonance was set at δ = -10.3 ppm.

Sample solution: 5% CD_3CD_2OD, 3% $(CD_3)_2SO$ in 1×PBS with 80 μM Aβ and 0.5 mM samples.

3 Results and Discussion

3.1 Chemistry

3.1.1 Isolation of Aβ aggregation inhibitor from *G. thunbergii*

The active compounds present in *G. thunbergii* were isolated via screening for Aβ aggregation inhibitory activity using an MSHTS system (Fig. 1).

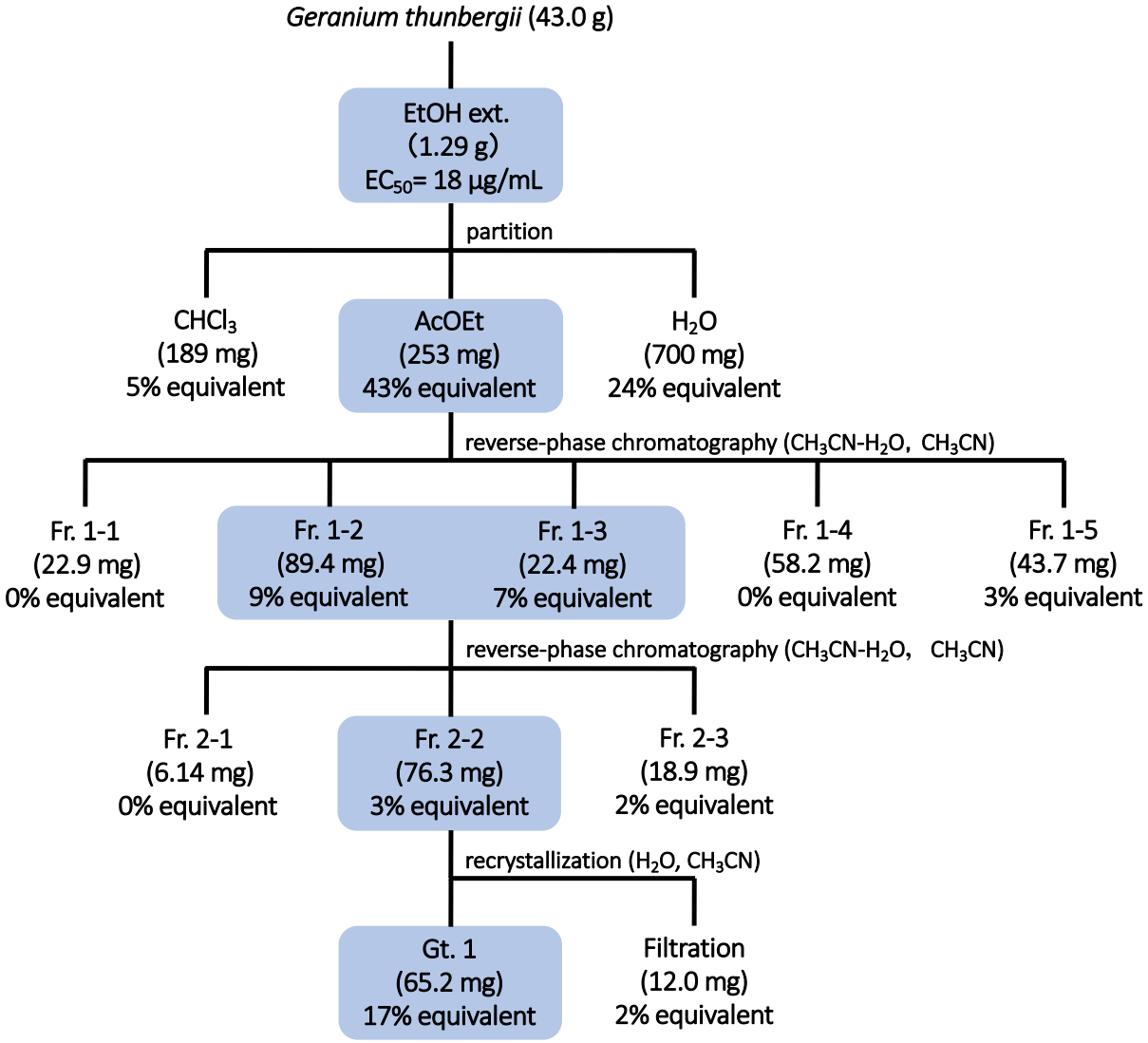

Fig. 1 Isolation of amyloid-beta aggregation inhibitor derived from *Geranium thunbergii*.

Here, the index of the active fraction was defined as the ratio based on the EC_{50} value of EtOH extract (18 μg/mL) and the contribution of each fraction to the activity of the EtOH extract (equivalent to %).

% Equivalent = Activity of EtOH extract (□g/mL) / Activity of each fraction (□g/mL) × 100 × Yield of fraction

Based on the successive liquid–liquid distribution of the EtOH extract using $CHCl_3$, AcOEt, and H_2O, the AcOEt layer showed the highest activity (43% equivalent). The AcOEt layer was repeatedly subjected to reverse-phase column chromatography to obtain Fr. 2-1, 2-2, and 2-3; Fr. 2-2 showed the best Aβ aggregation inhibitory activity (3% equivalent). Fr. 2-2 was re-crystalized using H_2O-CH_3CN to yield the active compound Gt. 1 (17% equivalent). The Aβ aggregation inhibitory activity of compound Gt. 1 was almost equivalent to that of rosmarinic acid (EC_{50} = 7 μg/mL), a reference compound. Thus, Gt. 1 may represent a useful lead compound for cognitive function improvement.

3.1.2 Structural analysis of active substances

Compound Gt 1 was a yellowish solid with a molecular weight of 951.4 $[M-H]^-$ based on electrospray ionization (ESI)-mass spectra. The ^{1}H-NMR spectrum confirmed that it was a mixture of Form A and Form B = 7:3 (Fig. 2).

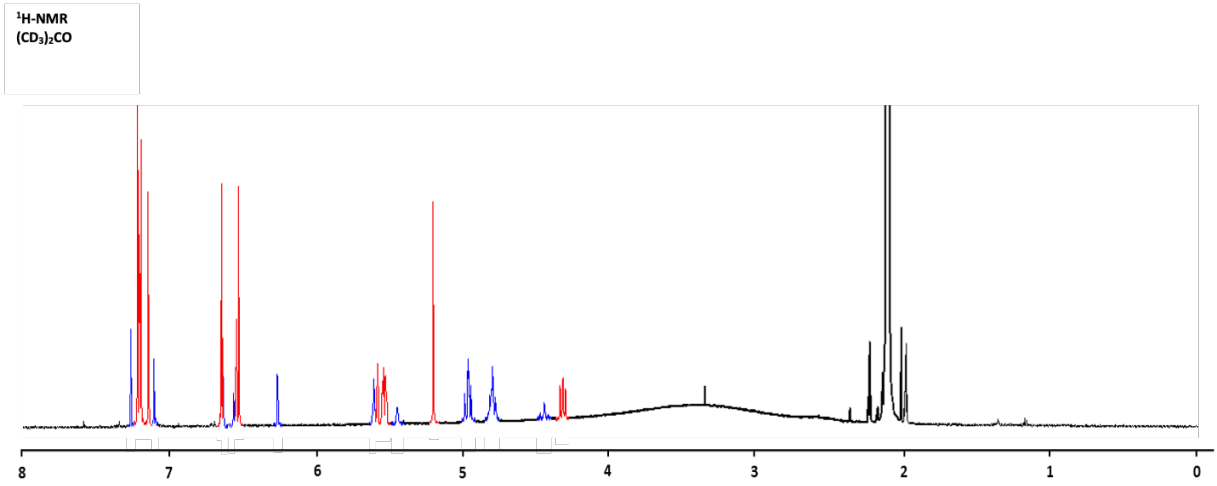

Fig. 2 ^{1}H-NMR spectrum of Gt. 1 in $(CD_3)_2CO$. Red- and blue- signals shown as geraniin Form A and B, respectively. ^{1}H-NMR, proton nuclear magnetic resonance.

Form A consisted of two equivalent aromatic methine hydrogens (δ_H: 7.20), three independent aromatic methine hydrogens (δ_H: 7.18, 7.13, and 6.63), one vinyl hydrogen (δ_H: 6.52), one methyl hydrogen (δ_H: 5.15), and seven oximethine hydrogens (δ_H: 6.53, 5.55, 5.51, 5.50, 4.94, 4.78, and 4.28). Form B had two equivalent aromatic methine hydrogens (δ_H: 7.19), three independent aromatic methine hydrogens (δ_H: 7.25, 7.08, and 6.62), one vinyl hydrogen (δ_H: 6.24), one methyl hydrogen (δ_H: 4.93), and seven aliphatic oximethine hydrogens (δ_H: 6.55, 5.59, 5.57, 5.42, 4.78, 4.75, and 4.40). Based on the ^{13}C-NMR and DEPT spectrum, Form A had 6 carbonyl carbons (δ_C: 191.8, 168.3, 166.1, 165.7, 165.4, and 164.7) and 2 vinyl carbons (δ_C: 154.7 and 128.6), and 2 equivalent aromatic quaternary carbons with polar substitutions (δ_C: 146.0), aromatic quaternary carbons with 10 independent polar substituents (δ_C: 145.8, 145.5, 145.1, 145.0, 144.6, 143.5, 139.8, 138.9, 137.9, and

136.5), 7 aromatic quaternary carbons (δ_C: 125.7, 124.8, 120.3, 119.7, 117.0, 115.8, and 115.2), 2 equivalent aromatic methine carbons (δ_C: 111.0), 3 independent aromatic methine carbons (δ_C: 113.4, 110.6, and 108.0), 8 oximethine carbons (δ_C: 96.3, 92.5, 90.7, 72.6, 69.9, 66.0, 63.7, and 63.3), and 1 methyl carbon (δ_C: 46.3). Form B had aromatic carbons with 6 carbonyl carbons (δ_C: 194.5, 168.2, 166.1, 165.7, 164.8, and 164.7), and 2 vinyl carbons (δ_C: 149.3 and 125.0), and 2 equivalent quartic carbon with polar substituents (δ_C: 146.0), aromatic quaternary carbon with 10 independent polar substituents (δ_C: 147.7, 147.3, 145.4, 145.2, 145.0, 144.7, 139.7, 137.8, 137.4, and 136.5), 7 aromatic quaternary carbons (δ_C: 125.5, 124.6, 120.3, 120.2, 117.2, 116.8, and 115.1), 2 equivalent aromatic methine carbons (δ_C: 110.7), 3 independent aromatic methine carbons (δ_C: 113.3, 110.3, and 108.7), 8 oximethine carbons (δ_C: 109.2, 92.4, 91.8, 73.3, 70.5, 67.0, 63.8, and 62.4), and 1 methyl carbon (δ_C: 52.0) (Table 1).

On comparison with data reported in literature,[22] Gt 1 was identified as geraniin (**1**) based on these ^{1}H-NMR and ^{13}C-NMR spectra (Fig. 3).

Table 1 NMR data of Gt 1

Position	δ_H, mult (J in Hz)		δc		Position	δ_H, mult (J in Hz)		δc	
	Form A	Form B	Form A	Form B		Form A	Form B	Form A	Form B
Glucose -1	6.53, bs	6.55, bs	90.7	91.8	Ring B-1'			115.2	115.1
Glucose -2	5.55, bs	5.57, bs	69.9	70.5	Ring B-2'			125.7	125.5
Glucose -3	5.50, bs	5.59, bs	63.3	62.4	Ring B-3'	6.63, s	6.62, s	108.0	108.7
Glucose -4	5.51, bs	5.42, bs	66.0	67.0	Ring B-4'			145.5	145.4
Glucose -5	4.78, bs	4.78, bs	72.6	73.3	Ring B-5'			136.5	136.5
Glucose -6a	4.28, dd	4.40, dd			Ring B-6'			145.0	145.0
	(12.3, 2.6)	(8.4, 2.3)	63.7	63.8					
Glucose -6b	4.94, bs	4.75, bs			Ring B-7'			168.3	168.2
Galloyl -1			120.3	120.3	Ring C-1'	5.15, s	4.93, s	46.3	52.0
Galloyl -2,	7.20, s	7.19, s	111.0	110.7	Ring C-2'			154.7	149.3
Galloyl -3, 5			146.0	146.0	Ring C-3'	6.52, s	6.24, d (1.4	128.6	125.0
Galloyl -4			139.8	139.7	Ring C-4'			191.8	194.5
Galloyl -7			164.7	164.7	Ring C-5'			96.3	92.4
Ring A-1			117.0	116.8	Ring C-6'			92.5	109.2
Ring A-2			124.8	124.6	Ring C-7'			165.6	165.7
Ring A-3	7.13, s	7.08, s	111.6	110.3	Ring D-1"			115.8	120.2
Ring A-4			144.6	144.7	Ring D-2"			119.7	117.2
Ring A-5			137.9	137.8	Ring D-3"	7.18, s	7.25, s	113.4	113.3
Ring A-6			145.1	145.2	Ring D-4"			145.8	147.7
Ring A-7			166.1	166.1	Ring D-5"			138.9	137.4
					Ring D-6"			143.5	147.3
					Ring D-7"			165.4	164.8

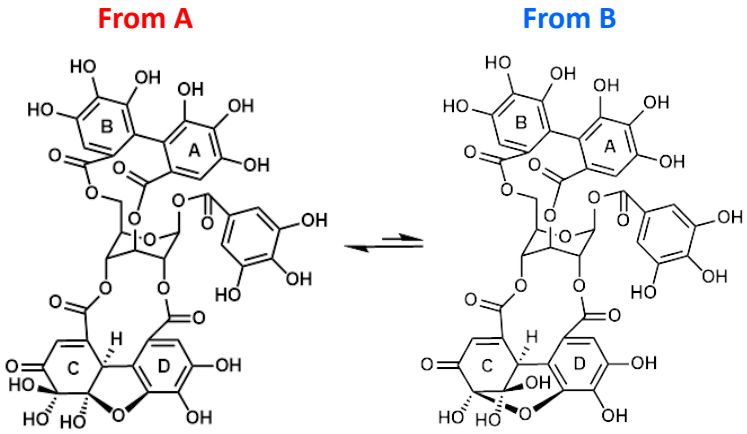

Fig. 3 Form A (Left) and form B (Right) of Geraniin (1).

3.2 Biological assays and mechanism of action

3.2.1 Degradation of geraniin under assay conditions for Aβ aggregation inhibitory activity

Geraniin (**1**) has been reported to exist in H_2O as an equilibrium mixture of two structures, Form A and Form B[25]. In this study, ^{1}H-NMR spectrum analysis under assay conditions (5% CD_3CD_2OD and 3% $(CD_3)_2SO$ in 1× PBS with 30 μM Aβ and 1,034 μM geraniin) revealed Form A and Form B = 1:6 immediately after dissolution. However, at 24 h of incubation, the geraniin signal was attenuated and multiple new signals (green signals) were observed, and the abundance ratio of Form A: Form B was 1: 3 (Fig. 4).

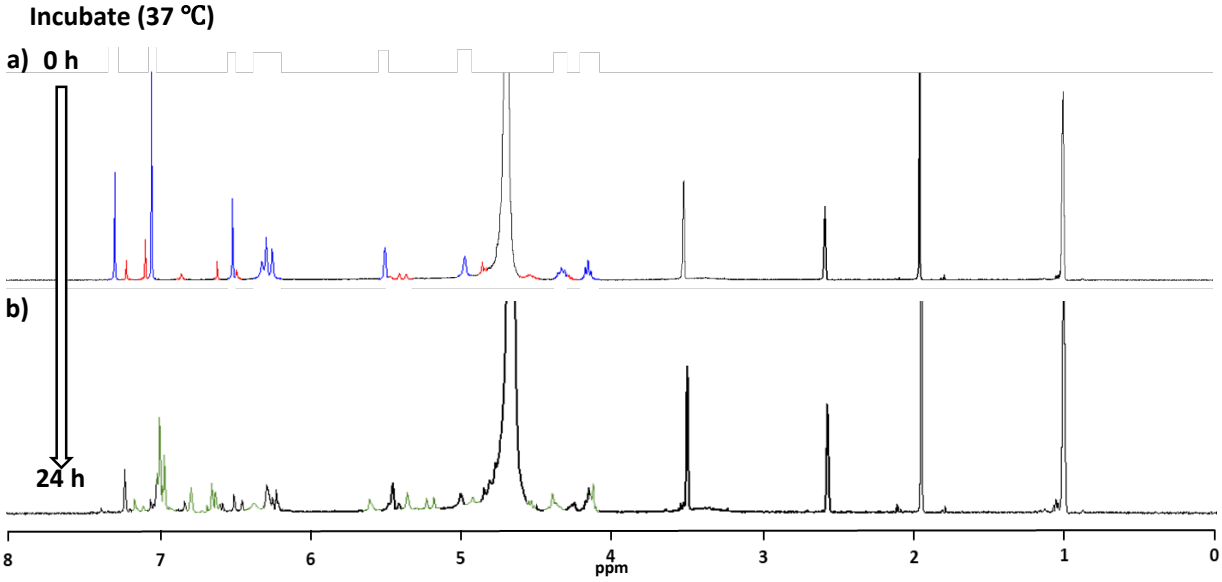

Fig. 4 ^{1}H-NMR spectra of geraniin (1) after incubation at 37 °C for (a) 0 h and (b) 24 h. Sample was prepared in assay conditions (5% CD_3CD_2OD and 3% $(CD_3)_2SO$ in 1× PBS with 30 μM Aβ and 1.0 mM geraniin)

3.2.2 Geraniin hydrolysis and decomposition products

The stability of geraniin (**1**) against hydrolysis was investigated by changing the phosphoric acid concentration, pH, and incubation temperature of the solution. Phosphate concentrations were set to D_2O only, 9.6 mM PBS, and 5.0 mM PBS, and their pH values were 5.9, 7.4, and 7.4, respectively. In addition, when ^{1}H-NMR analysis was performed at an incubation temperature of 4 °C and 37 °C, a new signal (green) was observed when pH was 7.4 and the incubation temperature was 37 °C regardless of the phosphoric acid concentration. It was evident that hydrolysis was in progress. Therefore, it was suggested that geraniin (**1**) maintains stability depending on the temperature and pH (Table 2).

Table 2 Stability test of geraniin (1)

Sample was measured in various conditions as follows: 1): D_2O with 1.0 mM geraniin (pH5.9), 2): 5% CD_3CD_2OD in 9.6 mM PBS with 1.0 mM geraniin (pH7.4), 3) 5% CD_3CD_2OD in 5 mM PBS with 1.0 mM geraniin(pH 7.4))

	D_2O	5% DMSO-d_6 / 9.6 mM PBS	5% DMSO-d_6 / 5 mM PBS
pH	5.9	7.4	
0 h	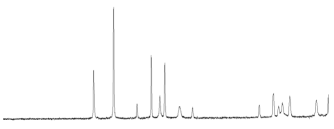	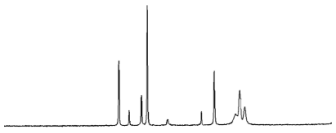	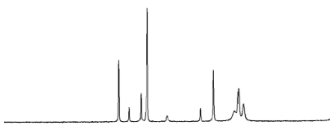
24 h 4℃	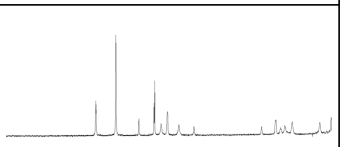	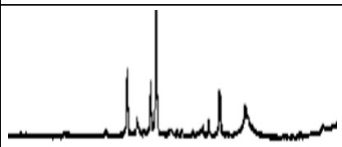	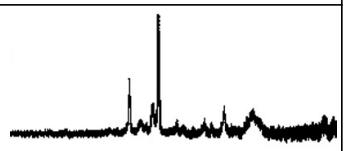
24 h 37℃	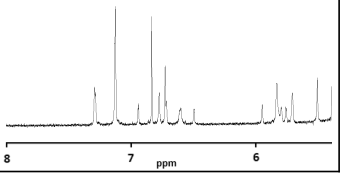	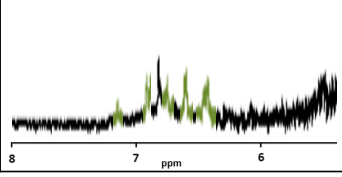	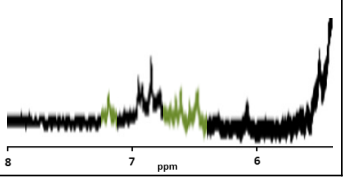

Geraniin hydrolysates include gallic acid (**2**), ellagic acid (**3**), hexahydrodiphenolic acid (**4**), and corilagin (**5**) (Fig. 5).[26] Therefore, the ^{1}H-NMR spectrum of the degradation product of geraniin was measured under assay conditions (5% CD_3CD_2OD, 3% $(CD_3)_2SO$ / 1× PBS) and compared with the ^{1}H-NMR spectrum of geraniin after 24 h of incubation (Fig. 6). Gallic acid (**2,** purple), ellagic acid (**3**, yellow), and corilagin (**5**, green) were observed among multiple new signals. Additionally, considering that the abundance ratio of Form A and Form B was initially 1: 6, but 24 hours after the hydrolysis reaction, it became 1: 3, the hydrolysis reaction rate of Form B was faster than Form A, and Form B was structurally and relatively more unstable (Fig. 4).

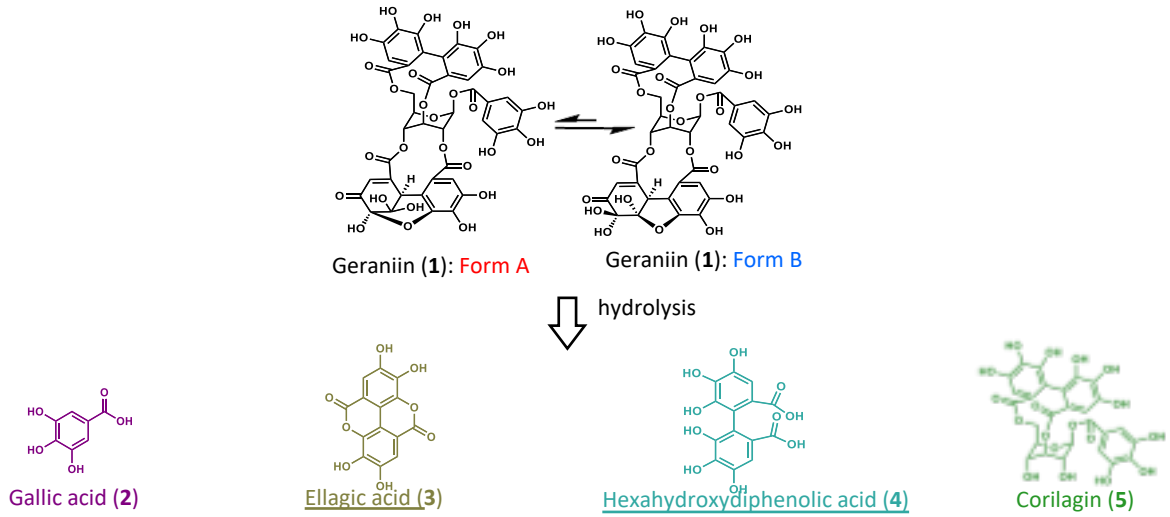

Fig. 5 Hydrolysis of geraniin in buffer (5% CD_3CD_2OD, 3% $(CD_3)_2SO$ / 1× phosphate-buffered saline)

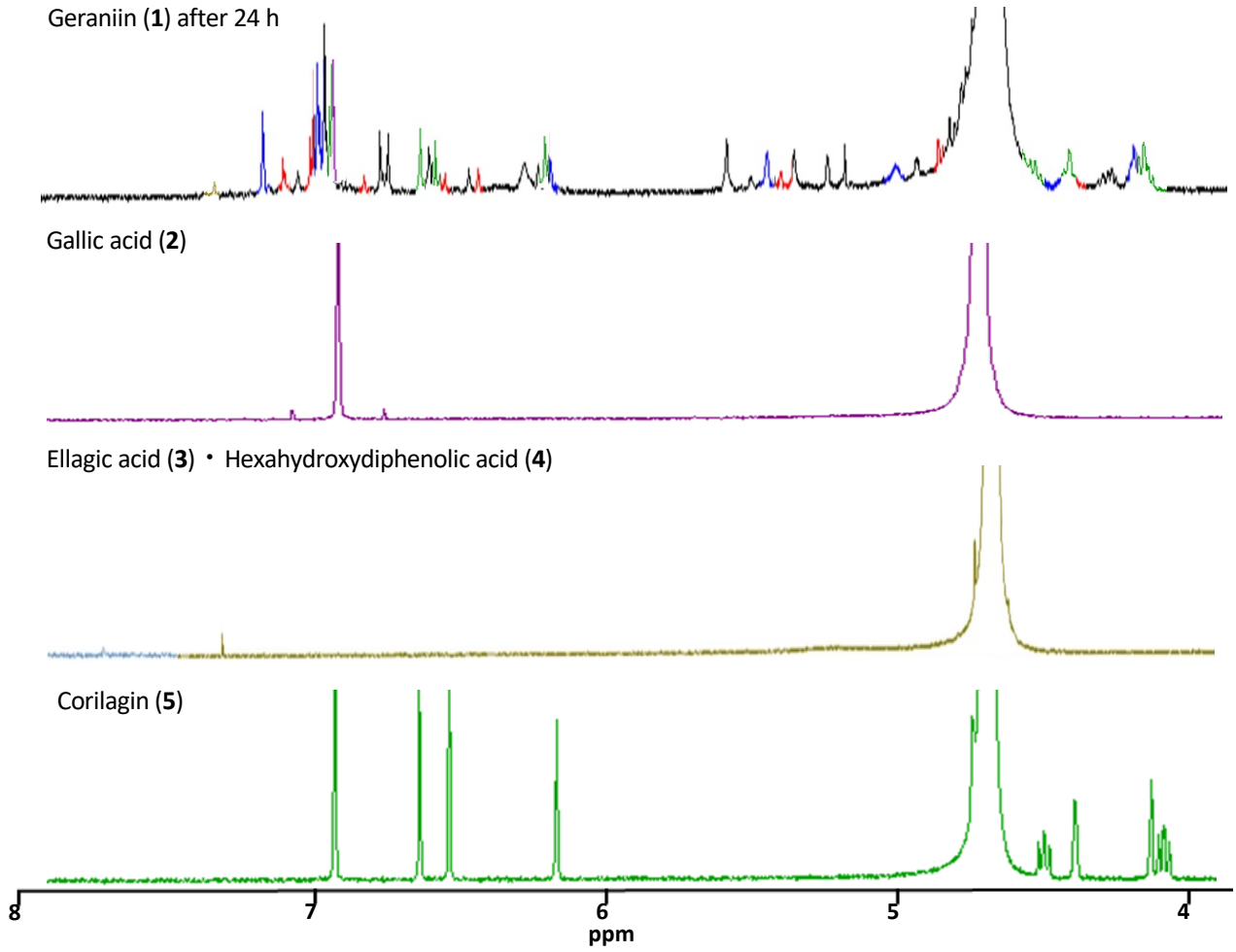

Fig. 6 Comparison of proton nuclear magnetic resonance spectra between hydrolysates of geraniin (1).

3.2.3 Activity contribution of geraniin (**1**) and its decomposition products (**2, 3,** and **5**)

Since the signals of the three decomposition products were confirmed based on ^{1}H-NMR spectra, the activity contribution (%) of each component was calculated based on the Aβ aggregation inhibitory activity and the integrated value of these hydrolysates. Analysis of the Aβ aggregation inhibitory activity of geraniin (**1**), gallic acid (**2**), ellagic acid (**3**), and corilagin (**5**) based on the MSHTS[6] and the ThT[23] methods revealed that the EC_{50} values were 6.7, 3.2, 1.7×10^2, and 3.2 μg/mL based on MSHTS analysis and 10, 1.7, 6.0×10^3, and 8.9 μg/mL based on ThT analysis, respectively. Since the abundance ratios of geraniin (**1**) Form A, geraniin Form B, gallic acid (**2**), ellagic acid (**3**), and corilagin (**5**) were 1.00, 0.35, 1.48, 0.13, and 0.41 based on the ^{1}H-NMR integration ratio, the molar abundance ratio was calculated as 0.1, 0.3, 0.44, 0.004, and 0.12, respectively. The activity contribution was calculated as gallic acid (**2**): 92 %, ellagic acid (**3**): 0.15 %, and corilagin (**5**): 25 % using the MSHTS method and gallic acid (**2**): 260 %, ellagic acid (**3**): < 0.01 %, and corilagin (**5**): 14 % using the ThT method; therefore, gallic acid (**2**) and corilagin (**5**) contributed to the apparent activity of geraniin (Table 3). Gallic acid (**2**) acts as an Aβ aggregation inhibitor[27–29] and fibril destabilization agent.[30] Moreover, it was reported that corilagin (**5**) protects PC12 cells against Aβ-induced damage and apoptosis.[31]

Activity contribution (%) = Apparent geraniin activity (EC_{50}) / EC_{50} × molar abundance × 100

Table 3 Contribution of the hydrolysates of geraniin (1) to the Aβ aggregation inhibitory effect via MSHTS and ThT analyses

	mole ratio	MSHTS		ThT	
		EC_{50} (μg/mL)	degree of contribution to activity (%)	EC_{50} (μg/mL)	degree of contribution to activity (%)
Geraniin (1)	-	6.7	-	10	-
Geraniin (1, Form A)	0.10	ND	ND	ND	ND
Geraniin (1, Form B)	0.30	ND	ND	ND	ND
Gallic acid (2)	0.44	3.2	92	1.7	260
Ellagic acid (3)	0.004	1.7×10^2	0.15	6.0×10^3	< 0.01
Hexahydroxydiphenic acid (4)	< 0.001	1.9×10^2	< 0.01	6.7×10^3	< 0.01
Corilagin (5)	0.12	3.2**	25	8.9**	14

**: $P < 0.01$ (Statistically significant level, Student's t-test). EC_{50}(MSHTS) *vs* EC_{50} (ThT)

Different results were obtained between the two evaluation methods, with no significant difference in the contribution of gallic acid (**2**) and significant differences in the contribution of corilagin (**5**). Since the MSHTS method targets late-stage aggregates of ≥1,000 peptides, whereas the ThT method targets early-stage aggregates of approximately 3–5 peptides,[32] it was suggested that the size of Aβ aggregates inhibited by gallic acid (**2**) and corilagin (**5**) was different: the inhibition of small peptide or large peptide aggregation was not verified for gallic acid (**2**); however, corilagin (**5**) inhibited the aggregation of mainly large peptide aggregates.

3.2.4 Examination of the interaction between the inhibitor and the soluble Aβ peptide

To determine the mechanism by which geraniin (**1**), gallic acid (**2**), and corilagin (**5**), which are mainly involved in the inhibition of Aβ aggregation by geraniin (**1**), interact with the Aβ peptide based on STD NMR spectra,[24] the ^{1}H-NMR spectra of geraniin (**1**), gallic acid (**2**), and corilagin (**5**) with Aβ (-) and without Aβ (+) and the STD NMR of Aβ (+) were measured (Table 4). Comparing the ^{1}H-NMR spectra of Aβ (-) and Aβ (+) of each substance showed that the chemical shift of the compound was moved upon addition of Aβ. Comparing the ^{1}H-NMR spectrum of Aβ (+) and the STD NMR of Aβ (+) revealed a signal of corilagin (**5**) alone. This suggests that only corilagin (**5**) interacts with the soluble Aβ peptide, suggesting that gallic acid (**2**) inhibits the aggregation of large insoluble Aβ peptide aggregates and corilagin (**5**) inhibits the aggregation of small soluble Aβ peptide aggregates.

Table 4 Interaction between the inhibitor and Aβ peptide evaluated by STD-NMR

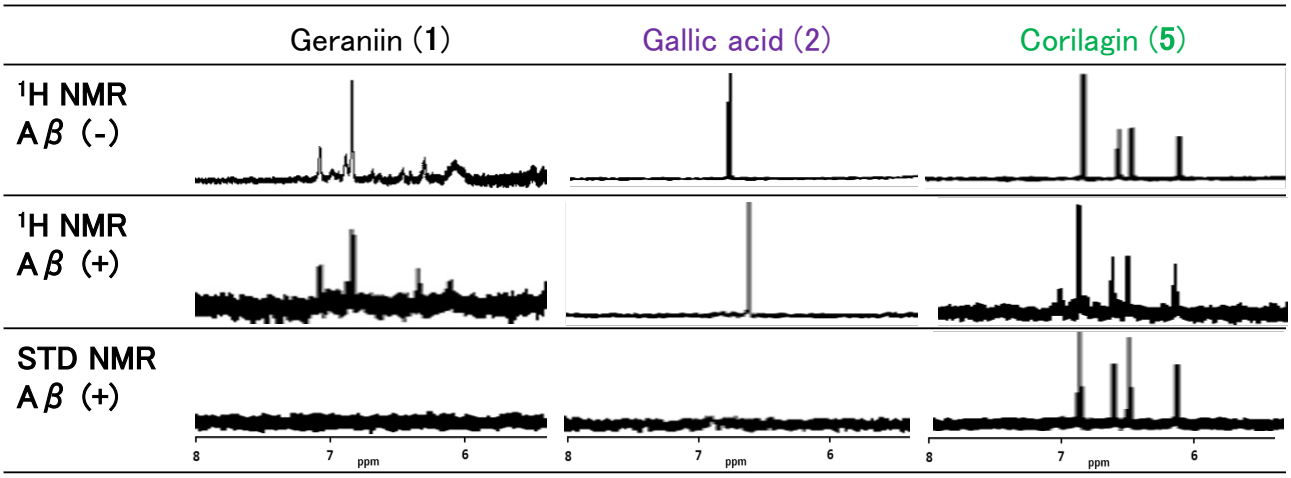

3 Conclusion

In this study, we investigated an Aβ aggregation inhibitor derived from *G. thunbergii*, which was found to be geraniin (**1**). Thus, the existing medicine *G. thunbergii* may be used for improving cognitive function from the viewpoint of drug repositioning. In addition, ^{1}H-NMR analysis revealed that the tannin geraniin (**1**) was hydrolysed under assay conditions. Therefore, the Aβ aggregation inhibitory activity of geraniin and its hydrolysates (gallic acid (**2**), ellagic acid (**3**), hexahydrodiphenolic acid (**4**), corilagin (**5**)) was evaluated, and the contribution of each activity was calculated based on the integrated value of each substance in ^{1}H-NMR. Gallic acid (**2**) and corilagin (**5**) were found to contribute to the Aβ aggregation inhibitory activity. This result was also supported by STD-NMR spectra between these compounds and Aβ. Therefore, substances that are unstable under biological conditions may have adverse effects[33, 34] and beneficial effects exerted by their degradation products. An extensive evaluation of the active compounds is necessary. Further studies should investigate relatively more effective analogues and elucidate the mechanism of action of these compounds.

Acknowledgements
The NMR experiments were performed at Hokkaido University Advanced NMR Facility, a member of NMR Platform (K. Uwai).

Funding
This work was supported by JSPS KAKENHI Grant Number 19K05728 (K. Uwai).

Declaration of competing interest
The authors declare that they have no known competing financial interests or personal relationships that could have appeared to influence the work reported in this paper.

References
1. Jack Jr CR, Knopman DS, Jagust WJ, Shaw LM, Aisen PS, Weiner MW, Petersen RC, Trojanowski JQ. Hypothetical model of dynamic biomarkers of the Alzheimer's pathological cascade. *Lancet Neurol*. 2010; 9: 119-128. https://doi.org/10.1016/S1474-4422(09)70299-6
2. Peters R, Anderson CS. Advancing dementia prevention through effective blood pressure control. *Lancet Neurol*. 2020; 19(1): 25-27. https://doi.org/10.1016/S1474-4422(19)30407-7
3. Yiannopoulou KG, Papageorgiou SG. Current and future treatments for Alzheimer's disease. *Ther Adv Neurol Disord.* 2013; 6(1): 19–33. https://doi.org/10.1177/ 1756285612461679
4. Hardy J, Selkoe DJ. The amyloid hypothesis of Alzheimer's disease: progress and problems on the road to therapeutics. *Science*. 2002; 297: 353-356. https://doi.org/10.1126/science.1072994
5. Porat Y, Abramowitz A, Gazit E. Inhibition of amyloid fibril formation by polyphenols: structural similarity and aromatic interactions as a common inhibition mechanism. *Chem Biol Drug Des*. 2006; 67: 27-37. https://doi.org/10.1111/j.1747-0285.2005.00318.x.
6. Ishigaki Y, Tanaka H, Akama H, Ogara T, Uwai K, Tokuraku K. A microliter-scale high-throughput screening system with quantum-dot nanoprobes for amyloid-β aggregation inhibitors. *PlosOne.* 2013; 8 (8): e72992. https://doi.org/10.1371/journal.pone.0072992.
7. Ogara T, Takahashi T, Yasui H, Uwai K, Tokuraku K. Evaluation of the effects of amyloid β aggregation from seaweed extracts by a microliter-scale high-throughput screening system with a quantum dot nanoprobe. *J Biosci Bioeng.* 2015; 120 (1): 45-50. https://doi.org/10.1016/j.jbiosc.2014.11.018
8. Taguchi R, Hatayama K, Takahashi T, Hayashi T, Sato Y, Sato D, Ohta, K Nakano H, Seki C, Endo Y, Tokuraku K, Uwai K. Structure-activity relations of rosmarinic acid derivatives for the amyloid β aggregation inhibition and antioxidant properties. *Eur J Med Chem.* 2017; 138: 1066-1075. https://doi.org/10.1016/j.ejmech.2017.07.026
9. Sasaki R, Tainaka R, Ando Y, Hashi Y, Virupaksha DH, Suga Y, Murai Y, Anetai M, Monde K, Ota K, Ito I, Kikuchi H, Oshima Y, Endo Y, Nakao H, Sakono M, Uwai K, Tokuraku K. An automated microliter-scale high-throughput screening system (MSHTS) for real-time monitoring of protein aggregation using quantum-dot nanoprobes. *Scientific Reports.* 2019; 9: Article number 2587. https://doi.org/10.1038/s41598-019-38958-0

10. Deepak HV, Swamy MM, Murai Y, Suga Y, Anetai M, Yo T, Kuragano M, Uwai K, Tokuraku K, Monde K. Daurichromenic Acid from the Chinese Traditional Medicinal Plant *Rhododendron dauricum* Inhibits Sphingomyelin Synthase and Aβ Aggregation. *Molecules*. 2020; 25: 4077. https://doi.org/10.3390/molecules25184077
11. Cho S. Use of geranium herb. *Sogo Rinsho (Clinic All-Round)*. 2004; 53(12): 3092-3096.
12. Okuda T, Nayeshiro H, Seno K. Structure of geranin in the equilibrium state. *Tetrahedron Lett.* 1977; 50: 4421-4424. https://doi.org/10.1016/S0040-4039(01)83525-5
13. Taniguchi S, Nagano R, Bao L, Kuroda T, Ito H, Hatano T. Furosonin, a novel hydrolyzable tannin from geranium thunbergia. *Heterocycles*. 201; 86: 1525-1532. https://doi.org/10.3987/COM-12-S(N)65
14. Youn K, Jun M. *In Vitro* BACE1 Inhibitory Activity of Geraniin and Corilagin from *Geranium thunbergia*. *Planta Med*. 201; 79 (12): 1038-1042. https://doi.org/10.1055/s-0032-1328769
15. Okuda T, Yahida T, Mori K. Brevifolin, corilagin and other phenols from Geranium thunbergia. *Phytochemistry*. 1975; 14: 1877-1878. https://doi.org/10.1016/0031-9422(75)85321-0
16. Liu QH, Woo ER. Inhibitory Activity of IL-6 Production by Flavonoids and Phenolic Compounds from Geranium thunbergia. *Nat Prod Sci.* 2008; 14: 16-20.
17. Yazaki K, Yoshida T, Okuda T. Tannin production in cell suspension cultures of *Geranium thunbergia*. *Phytochemistry*. 1991; 30: 501-503. https://doi.org/10.1016/0031-9422(91)83714-V
18. Okuda T, Mori K, Hayatsu H. Inhibitory effect of tannins on direct-acting mutagens. *Chem Pharm Bull*. 1984; 32: 3755-3758. https://doi.org/10.1248/cpb.32.3755
19. Ito H, Hatano T, Namba O, Okuda T, Shirono T, Okuda T, Yoshida T. Constituents of *Geranium thunbergii* SIEB. et ZUCC. XV. Modified Dehydroellagitannins, Geraniinic Acids B and C, and Phyllanthusiin F. *Chem Pharm Bull.* 1999; 47: 1148-1151. https://doi.org/10.1248/cpb.47.1148
20. Ito H. Metabolites of the Ellagitannin Geraniin and Their Antioxidant Activities. *Planta Medica*. 2011; 77: 1110-1115. https://doi.org/10.1055/s-0030-1270749
21. Pokharel YR, Liu QH, Aryal DK, Kim YG, Woo ER, Kang KW. 7,7'-Dihydroxy bursehernin inhibits the expression of inducible nitric oxide synthase through NF-kB DNA binding suppression. *Nitric Oxide*. 2007; 16: 274-285. https://doi.org/10.1016/j.niox.2006.10.006.
22. Sudjaroen Y, Hull WE, Erben G, Würtele G, Changbumrung S, Ulrich CM,[a] Owen RW. Isolation and characterization of ellagitannins as the major polyphenolic components of Longan (*Dimocarpus longan*Lour) seeds. *Phytochemistry*. 2012; 77: 226-237. https://doi.org/10.1016/j.phytochem.2011.12.008
23. LaVin H 3rd. Thioflavine T interaction with synthetic Alzheimer's disease beta-amyloid peptides: detection of amyloid aggregation in solution. *Protein Sci*. 1993; 2: 404-410. https://doi.org/10.1002/pro.5560020312
24. Mayer M, Meyer B. Characterization of Ligand Binding by Saturation Transfer Difference NMR Spectroscopy. *Angew Chem Int Ed*. 1999; 38: 1784-1788. https://doi.org/10.1002/(SICI)1521-3773(19990614)38:12<1784::AID-ANIE1784>3.0.CO;2-Q

25. Hatano T, Yoshida T, Shingu T, Okuda T. ^{13}C Nuclear Magnetic Resonance Spectra of Hydrolyzable Tannins. III. Tannins Having $^{1}C_4$ Glucose and C-Glucosidic Linkage. *Chem Pharm Bull*. 1988; 36: 3849-3856. https://doi.org/10.1248/cpb.36.3849
26. Okuda T, Yoshida T, Nayeshiro H. Constituents of Geranium thunbergii SIEB. et ZUCC. IV. Ellagitannins. (2). Structure of Geraniin. *Chem Pharm Bull.* 1977; 25: 1862-1869. https://doi.org/10.1248/cpb.25.1862
27. San Wong DY, IMusgrave IF, Harvey BS, Smid SD. Açaí (Euterpe oleraceae Mart.) berry extract exerts neuroprotective effects against β-amyloid exposure in vitro. *Neurosci Lett*. 2013; 556: 221–226. https://doi.org/10.1016/j.neulet.2013.10.027
28. Porzoor A, Alford B, Hügel HM, Grando D, Caine J, Macreadie I. Anti- amyloidogenic properties of some phenolic compounds. *Biomolecules*. 2015; 5: 505–527. https://doi.org/10.3390/biom5020505
29. Andrade S, Loureiro JA, Pereira MdC. Influence of *in vitro* neuronal membranes on the anti-amyloidogenic activity of gallic acid: Implication for the therapy of Alzheimer's disease. *Arch Biochem Biophys.* 2021; 711: 109022. https://doi.org/10.1016/j.abb.2021.109022
30. Yu M, Chen X, Liu J, Ma Q, Zhuo Z, Chen H, Zhou L, Yang S, Zheng L, Ning C, Xu J, Gao T, Hou ST. Gallic acid disruption of Aβ1–42 aggregation rescues cognitive decline of APP/PS1 double transgenic mouse. *Neurobiol Dis*. 2019; 124: 67–80. https://doi.org/10.1016/j.nbd.2018.11.009. Epub 2018 Nov 14.
31. Youn K, Lee S, Jeong WS, Ho CT, Jun M. Protective Role of Corilagin on Ab25–35-Induced Neurotoxicity: Suppression of NF-jB Signaling Pathway. *J Med Food*. 2016; 19 (10): 901-911. https://doi.org/10.1089/jmf.2016.3714
32. Biancalana M, Makabe K, Koide A, Koide S. Aromatic Cross-Strand Ladders Control the Structure and Stability of β-rich Peptide Self-Assembly Mimics. *J Mol Biol*. 2008; 383: 205-213. https://doi.org/10.1016/j.jmb.2008.08.031
33. Jaszczak-Wilke EWA, Polkowska Z, Koprowski M, Owsianik K, Mitchell AE, Balczewski P. Amygdalin: toxicity, anticancer activity and analytical procedures for its determination in plant seeds. Molecules. 2021; 26 (8): 2253. https://doi.org/10.3390/molecules26082253
34. Nagel D, Wallcave L, Toth B, Kupper R. Formation of methylhydrazine from acetaldehyde N-methyl-N-formylhydrazone, a component of Gyromitra esculenta. *Cancer Res*. 1977; 37(9): 3458-60.